Experimental determination of local Strain effect on InAs/GaAs self-organized quantum dots

H. L. Wang, F. H. Yang, S. L. Feng,* H. J. Zhu, D. Ning, H. Wang, and X. D. Wang
National Laboratory for Superlattices and Microstructures, Institute of Semiconductors, Chinese Academy of Sciences, P.O. Box 912, Beijing 100083, China

(Received 1 June 1999; revised manuscript received 26 August 1999)

The energy barrier at InAs/GaAs interface due to the built-in strain in self-organized system has been determined experimentally. Such a barrier has been predicted by previous theories. From the deep-level transient spectroscopy (DLTS) measurements, we have obtained the electron and hole energy levels of quantum dots $E_e^{\mathrm{QD}\rightarrow\mathrm{GaAs}}=0.13$ eV and $E_h^{\mathrm{QD}\rightarrow\mathrm{GaAs}}=0.09$ eV relative to the bulk unstrained GaAs band edges E_c and E_v. DLTS measurements have also provided evidence to the existence of the capture barriers of quantum dots for electron $E_{eB}=0.30$ eV and hole $E_{hB}=0.26$ eV. The barriers can be explained by the apexes appearing in the interface between InAs and GaAs caused by strain. Combining the photoluminescence results, the band structures of InAs and GaAs have been determined.

Over the years, InAs grown on GaAs(100) has become a well-established model system for the study of the low-dimensional structures in the case of highly lattice-mismatched semiconductors. For InAs/GaAs(100) the lattice mismatch is about 7%. The formation of dislocation-free coherent islands of InAs on the GaAs substrate has been observed and attributed to a transition from a two-dimensional growth mode to a three-dimensional one. The dislocation-free coherent islands [self-organized quantum dots (QD's)] have been attracting considerable interest due to their highly efficient radiation rate and potential device applications.[1–6]

In the absence of strain effects, the confining potential for an electron (hole) is a square well formed by the offset of the conduction (valence) band of InAs and GaAs. However, the study of the influence of strain on band structures of InAs/GaAs is complicated by the variations of the confining potentials from one conventional cubic unit cell to another due to the variations of the strain from cell to cell. In Refs. 7 and 8, M.A. Cusack, Briddon, and Jaros presented a calculation of the electronic structure of InAs/GaAs quantum dots that includes the microscopic details of the strain and the mixing between the light-hole and heavy-hole bulk bands, and accounts for the change in the effective masses due to strain. The results show that the compressive strain in the barrier shifts the GaAs conduction-band edge above the unstrained level. There exist apexes in the interface between InAs and GaAs in the plot of the confining potentials for electrons and holes along the growth direction. The apexes can form an energy barrier for carriers at the InAs/GaAs interface in a self-organized QD's system. In our previous work, we have proposed a method[9] of using deep-level transient spectroscopy (DLTS) to monitor the built-in strain in strained superlattices. Because of the localization behavior of the QD wave function, we have also successfully performed DLTS measurements on InAs/GaAs self-organized quantum dots systems.[10,11] In this paper, we perform the combined DLTS and photoluminescence (PL) measurements on the samples of InAs/GaAs multilayer QD systems and our experimental results demonstrate the existence of the energy barrier for carriers at the InAs/GaAs interface as predicted by theories.

The structures studied here were grown by molecular beam epitaxy using VG V80H MKII system. The substrates are n^+-GaAs(100). Growth rate is 1 μm/h for GaAs and 0.1 μm/h for InAs. Samples were grown as follows. First, a 1-μm Si-doped ($2\times10^{18}\,\mathrm{cm}^{-3}$) GaAs buffer layer was grown at 600 °C. Then temperature was lowered to 450 °C for subsequent growth. A spacer layer of GaAs (10 nm) and InAs (0.5 ML or 2.5 ML) was repeated five times. Then a 50-nm GaAs spacer layer was followed. The process of deposition (GaAs/InAs) layers followed by GaAs (50 nm) spacer layers was repeated five times. Finally, a GaAs (150 nm) cap layer was deposited. Samples can be divided into two series. Samples in series *A* (*n*-type) were doped with Si ($3\times10^{16}\,\mathrm{cm}^{-3}$) homogeneously. For the convenience of discussion, we denote the sample of 0.5-ML InAs as *N*-0.5 ML and that of 2.5-ML InAs as *N*-2.5 ML. Samples in series *B* (*p*-type) were doped with Be ($3\times10^{16}\,\mathrm{cm}^{-3}$) homogeneously except the top 50 nm of cap layer with the concentration $1\times10^{19}\,\mathrm{cm}^{-3}$ for the ohmic contact. We denote the sample of 0.5-ML InAs as *P*-0.5 ML and that of 2.5-ML InAs as *P*-2.5 ML. The growth was monitored by reflection high-energy electron diffraction (RHEED), and the QD nucleation was seen directly via the onset of a spotty RHEED pattern. QD's are formed in samples *N*-2.5 ML and *P*-2.5 ML, as their InAs coverage exceeds the critical layer (1.6 ML); QD's are not formed in samples *N*-0.5 ML and *P*-0.5 ML, as the InAs coverage is only 0.5 ML. The QD dimensions are typically 6 nm in height and about 10 nm in diameter in the lateral dimension, and the density is about $5\times10^{11}\,\mathrm{cm}^{-2}$.[12]

The purpose of this specially designed structure is two-fold: (1) to improve the quality of the QD's and to enhance the intensity of DLTS signals; (2) to suppress strain along the growth direction by adding the 50-nm GaAs spacer layers.[10] For samples in series *A*, we prepared the Schottky diode for the DLTS measurements by evaporating Au onto the GaAs caper layer. The back ohmic contact was formed by alloying In onto the n^+-GaAs substrate; for series *B*, the samples were directly grown into the *p-n* junction structure. We alloyed AuAgZn onto the GaAs caper layer and Au-

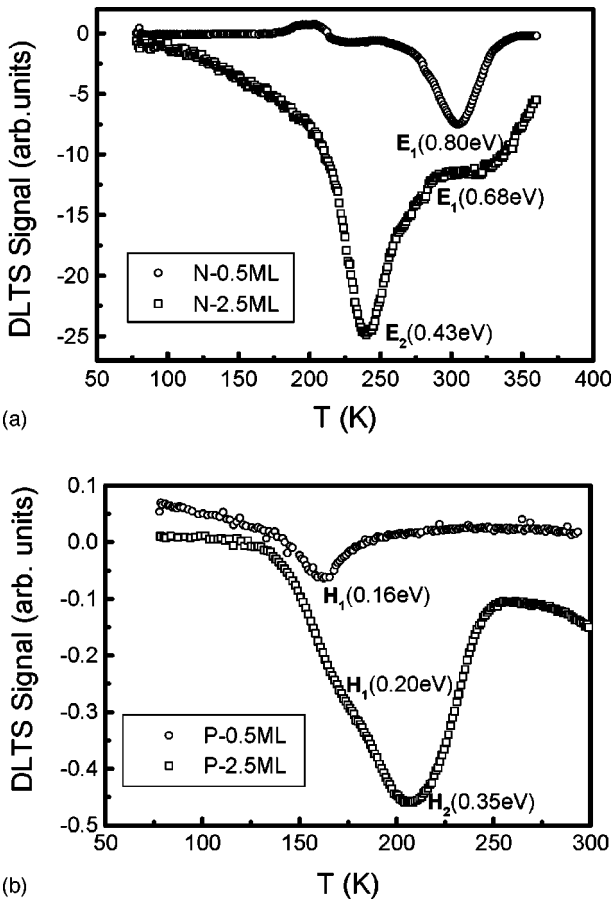

FIG. 1. Comparison of DLTS Curve between 0.5 and 2.5 ML sample [(a) doped with Si; (b) doped with Be]. All the spectra were recorded for the rate window of 8.28 ms, the filling pulse duration was 1 ms, the reverse bias was -1 V, and the pulse height was 0 V.

GeNi onto the n^+-GaAs substrate to form ohmic contacts. Then, we etched 1 μm to fabricate mesa diodes for the DLTS measurements.

DLTS measurements were carried out by using the Innovance *AB*-type deep-level transient spectroscopy. The range of temperature for measurements was 77-350 K. PL measurements were performed in a variable-temperature (7-300 K) closed cycle cryostat under the excitation of a 514.5 nm line of an argon laser. The signal from samples was dispersed by a Jobin-Yven HR250 monochromator and detected by a LN_2 cooled Ge detector.

All the DLTS measurements were performed under dark conditions. Before each scan, the sample was cooled down under zero bias and the measurements were made during the warm up cycle. The sample biasing conditions were obtained from the *C-V* measurements. Figure 1 shows the typical DLTS spectra of four samples under majority injection. In the samples of *N*-0.5 ML and *P*-0.5 ML without formed QD's only one clear peak was observed. From the activation plots of these signatures, we determined the apparent emission activation energies to be 0.80 eV for E_1 and 0.16 eV for H_1. In the samples of *N*-2.5 ML and *P*-2.5 ML with formed QD's two peaks were observed with one peak being stronger than the other. The inferred apparent emission activation energies are: $E_1=0.68$, $E_2=0.43$, $H_1=0.20$ and $H_2=0.35$ eV. The 2.5- and 0.5-ML InAs samples have the same structure and growth condition, with the only difference between them being that QD's are formed in the former and not in the latter. Only the samples of *N*-2.5 ML and *P*-2.5 ML with QD's exhibit the H_2 or E_2 peaks, indicating that the E_2 and H_2 peaks can be attributed to the energy levels of QD's. Otherwise, these peaks would also be observed in the samples without QD's, which is not the case. The peaks E_1 and H_1 have been observed in formed and unformed QD samples, so they can be attributed to deep centers in the bulk GaAs material, in which we are not interested.

With the variation of rate windows, the DLTS peak heights of E_2 and H_2 change distinctly, indicating that large capture barriers exist. The common procedure of measuring the capture parameters by changing the pulse width in getting the DLTS spectroscopy corresponds to a filling dynamic process. The capture kinetics are given by:

$$S(t_p)=S(0)+S(\infty)*[1-\exp(-C*t_p)], \tag{1}$$

where $S(t_p)$ is the peak height, $S(0)$ is the background signal, t_p is the carrier injection pulse width, $S(\infty)$ is the DLTS peak height when the quantum dots are fulfilled with carriers, $C=\sigma v n$ is the capture rate from which one can deduce the thermal capture cross section σ (v is the mean thermal velocity, and n the free carrier concentration).

A temperature dependence of capture rate C can be measured with variation of the rate window. We measured the dependence of the capture coefficient in the temperature range of 218–246 K for electron and 175–208 K for hole. The $\ln[1-S(t_P)/S(\infty)]$ versus t_p curves are shown in Fig. 2. The curves reflect that the capture process is an exponential one. Due to the fluctuation of QD sizes, the DLTS spectra of QD are broadened. The energy level broadening can cause the nonexponential transient. So, we see that the curves exists a little deviation from an exponential transient in the Fig. 2. The mean thermal velocity of carrier v can be calculated at a fixed temperature, and the free carrier concentration n approximately equals to the doped concentration. Thus a set of data on the capture cross sections versus temperature can be obtained.

The capture cross section that is thermal activated for many deep centers can be expressed as:

$$\sigma=\sigma_\infty \exp\left(-\frac{E_\sigma}{k_B T}\right), \tag{2}$$

where E_σ represents the capture barrier, σ_∞ is a constant independent of temperature, and k_B is the Boltzmann constant. The variations of σ with the inverse of temperature are given in Fig. 3. From it, we get the capture barrier $E_{eB}=0.30$ and $E_{hB}=0.26$ eV for electrons and holes, respectively. At the same time, the values of 1.66×10^{-15} cm^2 for electrons and 2.12×10^{-13} cm^2 for holes are determined for the pre-exponential factors σ_∞ from fitting the experimental data. Owing to the small temperature range in which peaks can be observed, the capture barrier associated with the capture cross section σ, measured from the slope of $\ln(\sigma)$ versus T^{-1}, often cannot be determined with a good accuracy.

Combining the capture barriers with the apparent emission activation energies, we can get the intrinsic emission activation energies (the binding energies) of QD's

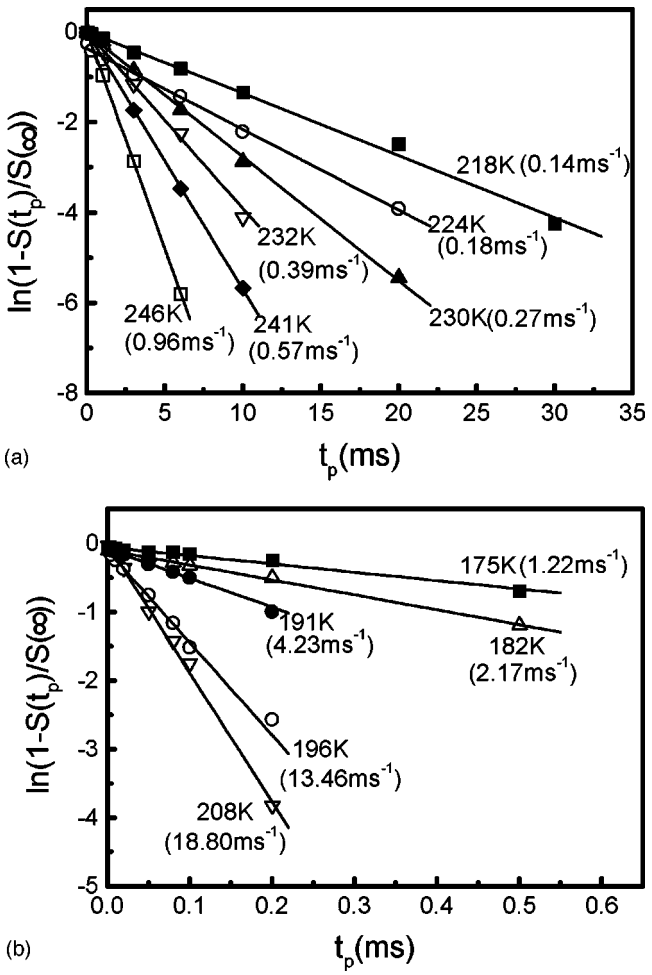

FIG. 2. Normalized DLTS signal amplitudes as a function of the activation pulse width at various temperature. (a) For the sample N-2.5 ML; (b) for the sample P-2.5 ML. The values in brackets are the capture rate obtained from the slope of related curve.

$E_h^{\mathrm{QD}\rightarrow\mathrm{GaAs}}=0.09\,\mathrm{eV}$ and $E_e^{\mathrm{QD}\rightarrow\mathrm{GaAs}}=0.13\,\mathrm{eV}$ for holes and electrons, respectively. If the base diameter is taken as 10 nm,[7] the theoretical values of the electronic levels of InAs/GaAs are about 0.12 eV for electrons and 0.1 eV for holes, with which our experimental results are in good agreement.

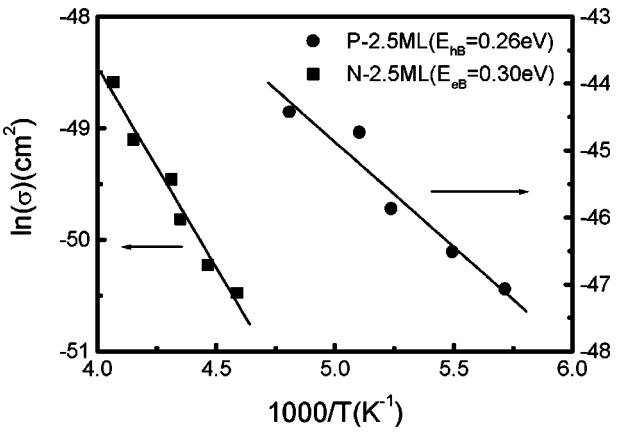

FIG. 3. Variations (logarithmic scale) of the capture cross section versus the inverse of the temperature. The rate window varies from 8.28 to 165.6 ms.

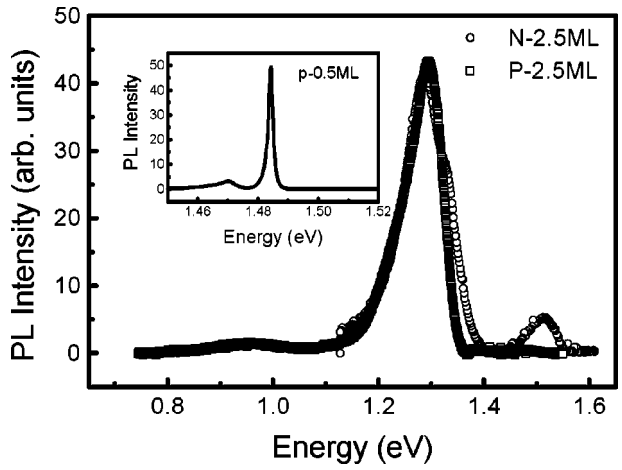

FIG. 4. The PL spectra of the sample N-2.5 ML and P-2.5 ML at the temperature of 10 K.

Moreover, our experimental results are in close agreement with many other published data on the electronic levels of QD's as measured by electric methods.[13,14]

We also performed the PL measurements for all the samples, with the spectra of the samples of N-2.5 ML and P-2.5 ML presented in Fig. 4. Both spectra are dominated by a strong luminescence peak related to the InAs QD's exciton transitions (1.29 eV). The same luminescence peak energy of QD's makes it easy to further analyze the results. It also shows the consistency of our sample growth. GaAs -related emissions (1.51 eV) are much weaker, even though GaAs has a much larger excitation volume. For comparison, the PL spectrum of P-0.5 ML is also shown in Fig. 4.

The full width at the half maximum (FWHM) of the PL for N-2.5 ML sample is 84.5 meV and for P-2.5 ML sample 75.5 meV. This indicates that there is a large size distribution of QD's in these samples. The obtained activation energies of QD's are average values. It is reasonable to take the range of the error values of the QD's localization energy as half of the FWHM (about 40 meV). The experimental error value of DLTS measurements is about k_BT (26 meV for room temperature). Thus, the estimated error on activation energy value is about 30–40 meV. According to linear regression in Fig. 3, the error of slope (E_B/k_B) for electron is 0.30 and for hole is 0.46. So, the error of capture barrier for electron is about 25 meV, for holes about 38 meV.

From the DLTS measurements, we have obtained the energy levels of QD's $E_e^{\mathrm{QD}\rightarrow\mathrm{GaAs}}=0.13\,\mathrm{eV}$ and $E_h^{\mathrm{QD}\rightarrow\mathrm{GaAS}}=0.09\,\mathrm{eV}$ relative to the top of the GaAs valence band E_V and the bottom of the GaAs conduction band E_C, respectively. From the PL measurements, we have obtained the energy difference of holes and electrons $E_{e\rightarrow h}^{\mathrm{QD}}=1.29\,\mathrm{eV}$ and the band gap $E_g^{\mathrm{GaAs}}=1.51\,\mathrm{eV}$. With these results, we have mapped out the energy band diagram in Fig. 5. We see that two results fit very well with each other and thus conclude that the barrier material for QD's is GaAs. When the electrons (holes) in QD's emit to the GaAs conduction (valence) band edge, they need to overcome the apparent emission activation energy $E_e(E_h)$. When the electrons (holes) in the GaAs conduction (valence) band edge are captured by the QD's they need to overcome the capture barrier $E_{eB}(E_{hB})$. The difference between $E_e(E_h)$ and $E_{eB}(E_{hB})$ is the energy

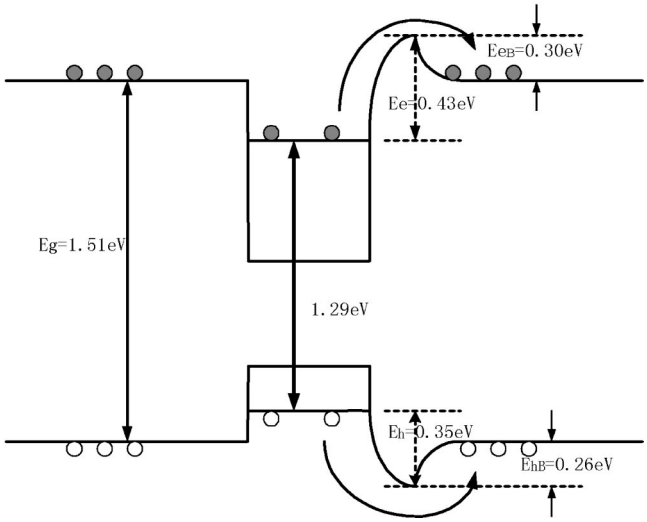

FIG. 5. Schematic band structure of InAs/GaAs self-organized quantum dots.

distance from QD levels to GaAs conduction (valence) band edge. The apexes in the interface between InAs and GaAs are caused by the strain, which we will discuss below in detail. It can form an energy barrier for carriers transferring between the well and barrier layers.

The DLTS spectrum is generated by voltage pulses, and differences in band bending should involved in Fig. 5 strictly. The electric field F varies linearly in the space charge region from zero at $x=W$, the limit of the space charge region, to typically $10^4\,\mathrm{V\,cm^{-1}}$ at $x=0$, the barrier interface (reverse biases are of the order of 1 V for space charge region of the order of 1 μm, with the doping concentration used, $n\sim 10^{16}\,\mathrm{cm^{-3}}$). The period of the superlattice is about 10 nm in our experiment. We can calculate that the band bending of each period is of the order of 1 meV. The value is far smaller than the capture barriers 0.30 eV for electrons or 0.26 eV for holes. The band-bending effects caused by electric field are not pronounced. So we can take it as flat band condition.

In the DLTS measurements, it is also seen that as the reverse bias is increased, the DLTS peaks shift slightly towards lower temperatures in the experiment. This trend indicates a little lowering of the emission barrier by the electric field. When the same bias condition is maintained during emission and only the filling pulse height is increased, the DLTS spectra show a progressive increase in the peak amplitude and is in accordance with increased filling of the dots. Therefore, we are able to vary the average number of electrons in the dots. The emission energy will be changed a little with the number of electrons in the dot. So, ensuring that the same average filling is maintained at all experiments is important. In our experimental conditions adopted, the emission spectra correspond to the dots having one electron or hole on the average. Although these phenomena are not the main theme of the present work, it should also be stressed that extreme care has to be taken while interpreting the experimental data.

We know that the InAs islands act as potential wells for charge carriers. The well profiles are given by the offset between the band edges in unstrained InAs and GaAs. The effect of strain on the confining potential profile was determined in Refs. 7 and 8. With strain taken into account, apexes appear in the GaAs side of the InAs/GaAs interface. Therefore, the electrons from conduction band (or the holes from the valence band) need to overcome the apex if they are to be captured by QD's. The apexes form the barriers for carriers being captured by QD's. Using the DLTS technique, we have determined the values of the barriers for both electrons and holes. Although the QD's are rather efficiently radiative and optical devices have been successfully demonstrated, it does not exclude the existence of a very large capture barrier of QD's. The capture barriers investigated in our experiments are those barriers that electrons or holes need to overcome before being captured from GaAs layers by QD's.

From the values of barriers, we can estimate the change of the lattice constant due to strain. When InAs was deposited on GaAs, the lattice constant of GaAs was compressed in growth direction and elongated in the perpendicular direction. Here, we are only concerned with the change in the growth direction. Gap energies when plotted as a function of the relative variation of lattice constant $\Delta a/a_0$ display an essentially linear dependence. Here, Δa can be calculated by using the Murnaghan equation of state[15]

$$P=(B_0/B_0')\{[a_0/a(p)]^{3B'_0}-1\} \tag{3}$$

with isothermal bulk modulus $B_0=74.66\,\mathrm{Gpa}$ and its pressure derivative $B_0'=4.67$. For GaAs, the pressure dependence of the direct energy gap is given by $dE_{g,dir}/dp=10.73\,\mathrm{meV/kbar}$. When the variation of band gap of GaAs is 560 meV, the equivalent strain pressure P is 52.19 kbar. Using these parameters, we get $a_0/a_{(p)}=1.02$. Based on the foregoing discussion, a method that determines the longitudinal strain profile in the strained structure is given by the stress effect on the deep levels.

In conclusion, we have determined experimentally the energy barriers at InAs/GaAs interface due to the built-in strain in self-organized systems, which have been predicted by previous theories. DLTS measurements have shown the existence of the capture barriers of quantum dots for electrons $E_{eB}=0.30\,\mathrm{eV}$ and holes $E_{hB}=0.26\,\mathrm{eV}$. The barriers can be explained by the apexes appearing at the interface between InAs and GaAs due to strain. From the PL measurements we have obtained the energy difference of holes and electrons $E_{e\to h}^{\mathrm{QD}}=1.29\,\mathrm{eV}$ and the band gap $E_g^{\mathrm{GaAs}}=1.51\,\mathrm{eV}$. With these results, the band structures of InAs and GaAs have been mapped out.

This work was supported by the National Sciences Foundation of China and the State Climbing Program for Basic Research.

*Author to whom correspondence should be addressed. FAX: (8610) 62324752. Electronic address: fengsl@red.semi.ac.cn

[1] Y. Arakawa and H. Sakaki, Appl. Phys. Lett. **40**, 939 (1982).
[2] M. Grundmann, O. Stier, and D. Bimberg, Phys. Rev. B **52**, 11 969 (1995).
[3] K. H. Schmidt, G. Mederiros-Ribeiro, M. Oestreich, P. M. Petroff, and G. H. Dohler, Phys. Rev. B **54**, 11 346 (1996).
[4] Z. Y. Xu, Z. D. Lu, X. P. Yang, Z. L. Yuan, B. Z. Zheng, and J. Z. Xu, Phys. Rev. B **54**, 11 528 (1996).
[5] R. C. Ashoori, H. L. Stormer, J. S. Weiner, L. N. Pfeiffer, K. W. Baldwin, and K. W. West, Phys. Rev. Lett. **71**, 613 (1993).
[6] H. Drexler, D. Leonard, W. Hansen, J. P. Kotthaus, and P. M. Petroff, Phys. Rev. Lett. **73**, 2252 (1994).
[7] M. A. Cusack, P. R. Briddon, and M. Jaros, Phys. Rev. B **54**, R2300 (1996).
[8] M. A. Cusack, P. R. Briddon, and M. Jaros, Phys. Rev. B **56**, 4047 (1997).
[9] J. F. Xiao, S. L. Feng, and C. S. Peng, Int. J. Infrared Millim. Waves **16**, 325 (1997) (in Chinese).
[10] F. Chen, S. L. Feng, X. Z. Yang, Q. Zhao, Z. M. Wang, and L. S. Wen, Phys. Low-Dimens. Semicond. Struct. **11/12**, 179 (1997).
[11] F. Chen, S. L. Feng, Qian Zhao, Z. M. Wang, X. Z. Yang, L. S. Weng, Superlattices Microstruct. **24**, 353 (1998).
[12] Z. M. Wang, S. L. Feng, X. P. Yang, Y. M. Deng, Z. D. Lu, X. Y. Xu, Z. G. Chen, H. Z. Zheng, P. D. Han, F. L. Wang, and X. F. Duan, Phys. Low-Dimens. Semicond. Struct. **11/12**, 213 (1997).
[13] P. N. Brunkov, S. Konnikov, V. M. Ustinov, A. E. Zhokov, A. Yu. Egorov, M. V. Maksimov, N. N. Ledentsov, and P. S. Kop'ev, Fiz. Tekh. Polugrovodn. **30**, 924 (1996), [Semiconductors **30**, 492 (1996)].
[14] G. Medeiros-Rebeiro, D. Leonard, and P. M. Petroff, Appl. Phys. Lett. **66**, 1767 (1995).
[15] H. J. Mcskimin and P. Andreatch, J. Appl. Phys. **34**, 651 (1963).